ELSEVIER

Journal of Wind Engineering
and Industrial Aerodynamics 72 (1997) 323–333

JOURNAL OF
wind engineering
AND
industrial
aerodynamics

Modelling of base-isolated buildings with passive dampers under winds

Ahsan Kareem

NatHaz Modelling Laboratory, Department of Civil Engineering and Geological Sciences, University of Notre Dame, Notre Dame, IN 46556-0767, USA

Abstract

This paper presents dynamic analysis of base-isolated buildings under wind loads. Also considered here is the dynamics of base-isolated buildings with passive dampers attached at the building base and/or top. Analysis is performed using a state-space approach which models wind velocities as a coupled set of linear stochastic differential equations. Various building-damper configurations are studied to determine effects of the type of dampers and their placement on the building response. A parameter study involving building and base-isolation properties is conducted to gain insight into their influence on building response.

Keywords: Base-isolation; Wind engineering; Earthquakes; Tuned mass damper; Dynamics; Random vibration

1. Introduction

The base-isolated systems to protect structures against earthquake excitations are receiving increasing attention in design and construction of buildings in seismic zones. Several such systems have been employed in buildings and a detailed review concerning the analysis and design of base-isolated structures is given by Kelly [1]. Additional studies concerning performance, evaluation of different systems and modelling for probabilistic analysis can be found, for example, in Ref. [2]. The base-isolation systems can be classified into three broad categories, i.e., pure-friction (P-F) system; laminated rubber bearings (LRB) system and resilient-friction base-isolator (R–FBI) system. Other systems involve the use of hysteretic dampers, or some combination of the isolation systems described. The sensitivity of a building with base-isolation system to wind loads is increased as base-isolation generally increases the horizontal flexibility of a structure. Limited studies have addressed the question of this increased sensitivity and its impact on building performance [3–5]. Kareem and DeKlotz [4] and Sinha and Li [6] have studied the response of base-isolated structures with dynamic absorbers.

PII S0167-6105(97)00232-8

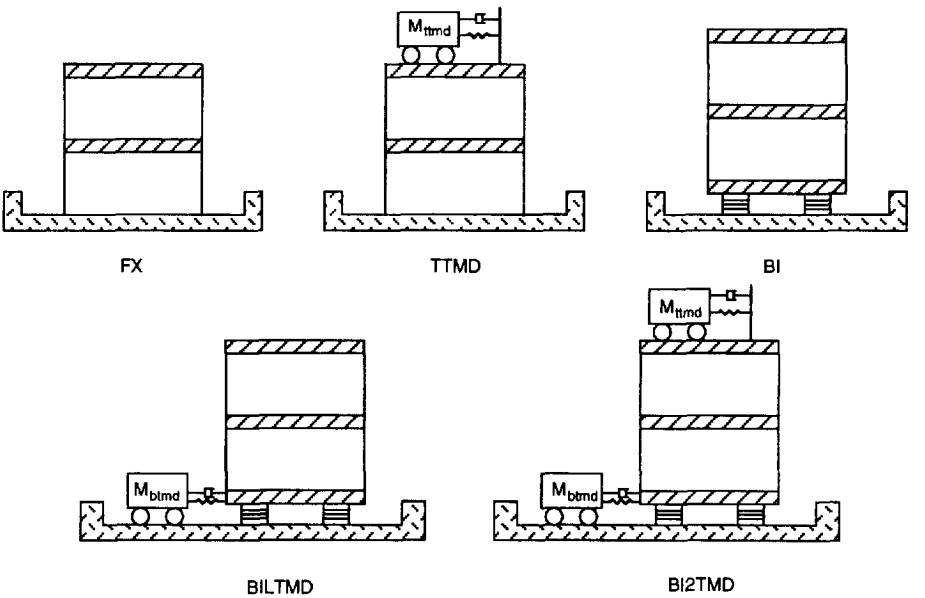

Fig. 1. Different building isolator–damper configurations.

This paper concerns the analysis of base-isolated buildings alone and with tuned mass dampers attached to the base and/or top of buildings subjected to the alongwind excitations [4]. The analysis is limited here to LRB system; however, the analysis scheme is equally applicable for other isolation systems by utilizing an equivalent linearization approach to account for nonlinearity. The top TMD (TTMD) is intended to control the building sway and the bottom TMD (BTMD) is included to protect the isolation system from excessive deformation and damage [7]. The TMD configurations examined in this study are shown in Fig. 1.

2. Modelling and analysis

2.1. System modelling

The equations of motion of a building excited by the alongwind loading is represented by a discretized lumped-mass system.

$$M\ddot{X}(t) + D\dot{X}(t) + KX(t) = F(t), \tag{1}$$

where $X(t)$ represents displacement vector, $F(t)$ the wind loading, and M, K and D represent the mass, stiffness, and damping matrices, respectively. The building is represented by five lumped masses. For the building with both TTMD and BTMD

the mass stiffness matrices are given by

$$M = \begin{bmatrix} m_{ttmd} & \{0\} & 0 & 0 \\ \{0\}^{\mathrm{T}} & M_{\mathrm{ss}} & \{0\}^{\mathrm{T}} & \{0\}^{\mathrm{T}} \\ 0 & \{0\} & M_{\mathrm{BI}} & 0 \\ 0 & \{0\} & 0 & m_{btmd} \end{bmatrix}$$

and

$$K = \begin{bmatrix} k_{ttmd} & k_{zt} & 0 & 0 \\ k_{zt}^{\mathrm{T}} & K_{\mathrm{ss}} & k_{zbi}^{\mathrm{T}} & \{0\}^{\mathrm{T}} \\ 0 & k_{zbi} & k_{\mathrm{BI}} - k_{45} + k_{btmd} & -k_{btmd} \\ 0 & \{0\} & k_{btmd} & k_{btmd} \end{bmatrix} \tag{2}$$

in which M_{ss} and K_{ss} represent original structural and mass and stiffness matrices; m_{ttmd}, k_{ttmd}, m_{btmd}, k_{btmd}, top and base TMD's masses and stiffnesses, k_{BI}, M_{BI} are the base-isolation stiffness and mass; k_{zt} is a row vector with zeros except the first element equal to $-k_{tt}$ and k_{zbi} is a row vector containing zeros except the last element being equal to k_{45}. The stiffness matrix K_{ss} also has the provision to include $P-\Delta$ effects. The shear rigidity and the number of bearings to be used is determined from the desired isolation period [1]:

$$T_{\mathrm{b}} = 2\pi \left[\frac{W_{\mathrm{b}}}{K_{\mathrm{h}} g}\right]^{1/2}, \tag{3}$$

where W_{b} is the static load on a bearing and $k_{\mathrm{h}} = GA_{\mathrm{s}}/L$, where GA_{s} and L represent shear rigidity and length of an individual bearing, respectively. The stiffness of the rubber bearing is reduced due to $P-\Delta$ effects [8]:

$$K_{\mathrm{h}} = \frac{GA_{\mathrm{s}}}{L}\left[1 + \frac{\dfrac{8}{\pi^2}\left(1 + \dfrac{P}{GA_{\mathrm{s}}}\right)^2}{\dfrac{\pi^2 EI}{GA_{\mathrm{s}}L^2} - \dfrac{P}{GA_{\mathrm{s}}}\left[1 + \dfrac{P}{GA_{\mathrm{s}}}\right]}\right]^{-1}, \tag{4}$$

where P is the compressive force and EI the flexural stiffness of the bearing.

For effective utilization of TMDs it is essential that these be tuned optimally. It is noted that for base-isolated buildings the tuned parameters i.e., frequency ratio and damper damping deviate from the values obtained from classical results for fixed base structures. In this study optimal values of Ω and ξ_{d} were determined for a range of buildings with fixed base and isolated base modelled as SDOF, MDOF with base and top TMDs. The results suggest that the optimal values agree for a single degree of freedom system model for fixed base with those reported by Warburton [9] and Kareem [10]. The optimal values for the MDOF fixed base case departed from the

SDOF case. However, for the base isolated with TMDs the results deviated from conventional values customarily used for sizing dampers. The introduction of base-isolation into the system fundamentally changes the distribution of structural parameters, resulting in non-uniform values of ξ_d and Ω for differing building heights. As a consequence, the optimization of TMD parameters for each base-isolated structural system must be performed individually [11].

3. Wind loading

Typically, a structure exposed to wind experiences alongwind, acrosswind, and torsional motions. The alongwind response is due to forces parallel to the mean wind and are described adequately by strip and quasi-steady theories. The objective of this study is to examine the dynamics of base-isolated buildings; therefore, it is restricted to the alongwind response only. Similar trends in the results are expected for the other wind directions. The power spectral density matrix of wind excitations at different levels based on the quasi-steady and strip theories can be easily formulated [11].

A state-space format is utilized to express the buffeting loading in the alongwind direction described by a cross spectral density matrix. In this approach the wind velocities are the output of a state-space filter for which the input is a vector of white-noise processes with unit power spectral density [12, 4, 13]:

$$v(t) = Cw(t),$$

$$\dot{w}(t) = Aw(t) + B\xi(t), \tag{5}$$

where $v(t)$ is the wind velocity, $\xi(t)$ the white noise and A, B and C are the coefficient matrices. In Fig. 2, a schematic description of this model is presented. The correlated wind velocities at five levels are simulated utilizing a prescribed coherence structure. The associated time histories of fluctuating force are derived from the following:

$$f(t) = GCw(t), \quad G = \rho C_D[A_{B_i}\bar{V}_i], \tag{6}$$

in which C and $w(t)$ have been defined previously and A_{B_i} is the building area at ith level and $\bar{V}_i$ the mean wind velocity at ith level. In order to perform this simulation to generate loads, matrices A, B and C need to be estimated. In this regard, first the auto- and cross-spectral density functions of wind field are approximated by rational functions to facilitate the factorization of the spectral matrix [14]. In the Laplace domain the spectral matrix can be factorized as

$$\boldsymbol{S}_{ff}(s) = \boldsymbol{H}(-s)\boldsymbol{H}^*(s). \tag{7}$$

The transfer function $\boldsymbol{H}(s)$ is then used to define a filter describing wind fluctuation model for which the input is a vector of unit intensity white noise processes and the output is a vector process with spectral matrix $\boldsymbol{S}_{ff}(w)$.

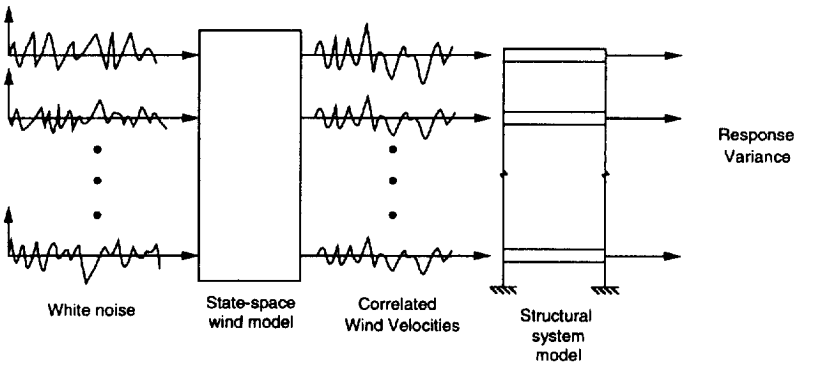

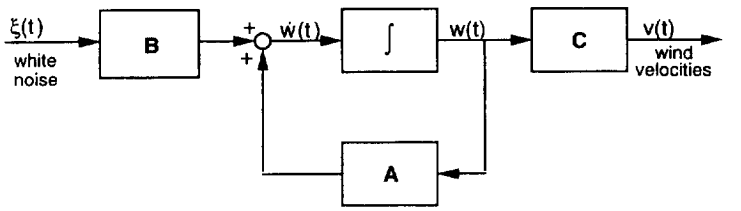

Fig. 2. Modelling of wind fluctuations and response.

The auto-spectrum at the ith node and cross-spectrum between the ith and jth modes are approximated by

$$S_{ff_{ii}} = \frac{\sum_{q=1}^{Q} a_{ii_q} s^{q-1}}{\prod_z (s + s_{zi}) + (-s + s_{zi})}; \quad \text{and} \quad S_{ff_{ij}} = \frac{\sum_{q=1}^{Q} a_{ij_q} s^{q-1}}{\prod_z (s + s_{zi})(-s + s_{zj})} \tag{8}$$

where a_{ij} and s_z are determined numerically such that the mean square error between the chosen function and the original spectrum becomes minimal over the entire frequency range. The number of parameters to be fitted, $z + q$, depends upon the desired degree of accuracy.

By the application of a series of similarity transformations of the power spectral density matrix of wind excitations, $S_{ff}(s)$, now approximated by a matrix of rational functions, a matrix transfer function, $H(s)$, is obtained:

$$[T_n(s) \ \ldots \ T_2(s) \ T_1(s)] S_{ff}(s) [T_1^{\mathrm{T}}(-s) T_2^{\mathrm{T}}(-s) \ \ldots \ T_n^{\mathrm{T}}(-s)] = I,$$

$$H(s) = T_1^{-1}(s) T_2^{-1}(s) \ \ldots \ T_n^{-1}(s), \tag{9}$$

where the T_i are transformation matrices and I is the identity matrix. A detailed description of this factorization is provided in Kareem and DeKlotz [4].

To find the A, B, and C matrices of Eq. (9), the minimal state-space realization of the matrix transfer function must be found such that

$$H(s) = C(sI - A)^{-1}B. \tag{10}$$

For wind force spectral densities generated based on the quasi-steady and strip theories, the following simplifications to the solution process have been found to provide satisfactory representation. The main simplification involves the rational functions used to approximate the power spectra:

$$S_{ff_{ii}} = \frac{a_{ii}}{(s + b_i)^2 + (-s + b_i)^2}, \qquad S_{ff_{ij}} = \frac{a_{ij}}{(s + b_i)^2(-s + b_j)^2}, \tag{11}$$

where the parameters a_{ij} and b_i are determined by a least-squares fit.

These rational functions take advantage of the method of factorization and of the nature of the relation between auto- and cross-spectra. The factorization of the spectral matrix and the determination of the minimal state-space realization of the resulting matrix transfer function are also simplified. Details of these procedures are given in Ref. [4].

The auto- and cross-power spectral densities of wind force fluctuations at various building levels are generated. These are plotted in Fig. 3 along with the corresponding target spectral descriptions based upon the quasi-steady and strip theories. As can be seen, the rational function approximations come extremely close to the original spectral descriptions except in the high-frequency range.

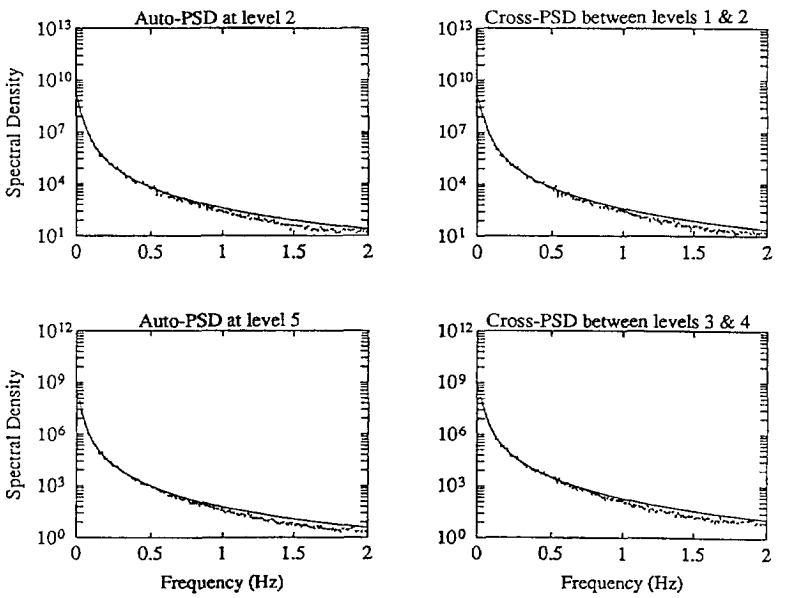

Fig. 3. Comparison of simulated and target spectral descriptions.

4. Building–TMD system response

The response statistics is obtained using a state-space formulation of the building–TMD–loading system in which the covariance matrix P is found by solving the following equation:

$$JP + PJ^{\mathrm{T}} = -Q,$$

where

$$J = \begin{bmatrix} 0 & I & 0 \\ -M^{-1}K & -M^{-1}D & M^{-1}GC \\ 0 & 0 & A \end{bmatrix} \text{ and } -Q = \begin{bmatrix} 0 & 0 \\ 0 & -BB^{\mathrm{T}} \end{bmatrix}. \tag{12}$$

Contained in the matrix P are the variances for x, $\dot{x}$, and w, the displacement, velocity, and state vectors, respectively, and their covariances. Eq. (11) is a Lyapunov equation, which can be solved using one of the several numerical algorithms available in the literature. A simple transformation is required to obtain the variances of the acceleration response given below [4]:

$$E[\ddot{X}\ddot{X}^{\mathrm{T}}] = E[UXX^{\mathrm{T}}U^{\mathrm{T}}] = UE[XX^{\mathrm{T}}]U^{\mathrm{T}} = UPU^{\mathrm{T}}, \tag{13}$$

where $X = [x\ \dot{x}\ w]^{\mathrm{T}}$, $P = E[XX^{\mathrm{T}}]$, $\ddot{x} = UX$ and $U = [-M^{-1}K : -M^{-1}D : M^{-1}GC]$.

5. Results and discussion

The description and results of several computer simulations, utilizing the models of structural components and the methods of analysis described previously, are now presented. The goal of the first study is to analyze the effectiveness of the proposed passive control system by determining the root mean square (RMS) response of the various structure–damper configurations. The validity of customary assumption based on classical damping for the various configurations is examined in the second investigation. The influence of $P-\Delta$ effects on the system response are examined. Additionally, a parameter study is performed to delineate the influence of certain properties of the structural system on building performance.

5.1. Building response

The first set of computer simulations involved determination of the RMS response of the FX (fixed base), BI (base-isolated), BILTMD (base-isolated lower TMD), BITTMDC (base-isolated top TMD), and BI2TMD (base-isolated both lower and top TMD) configurations (shown in Fig. 1) under alongwind loads. The $P-\Delta$ effects on both the rubber bearings and the superstructure are taken into account in this

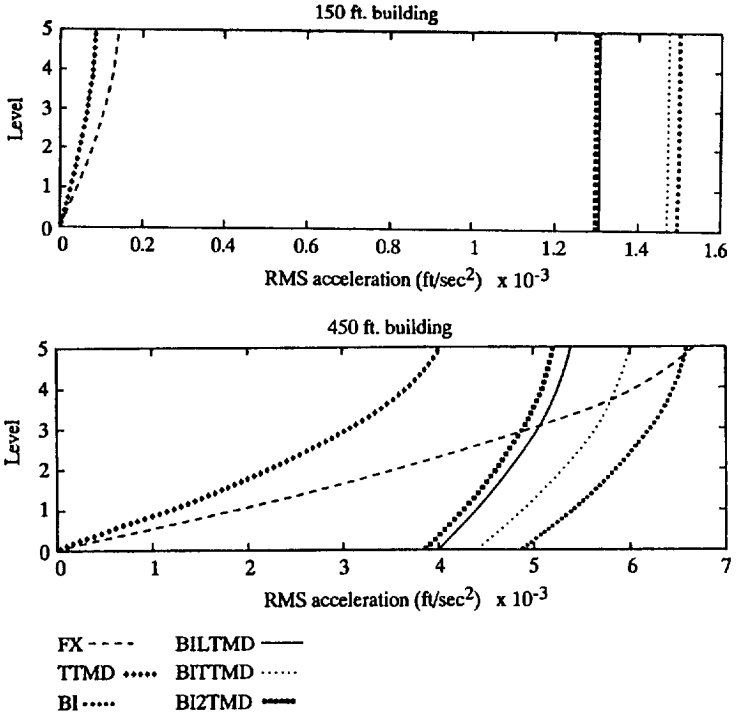

Fig. 4. RMS acceleration for different building configurations.

analysis. Each building system is condensed to five levels equally spaced, e.g., 150 ft building is represented by five levels of 30 ft height. The results are shown at each level. Fig. 4 shows the RMS acceleration response for the six configurations of the 450 and 150 ft buildings. A number of trends can be noted from these results. For the fixed base case, the top TMD is indeed effective in reducing acceleration levels of each building. In the case of base-isolated buildings, although the top TMD reduces the response, the lower TMD is significantly more effective. In the case of both the top and lower TMDs, the building response is further reduced; however, the improvement made in comparison with the lower TMD alone is not that significant. These trends are present in all building cases, whereas the quantitative changes in response are influenced by the relative flexibility of the building. Nonetheless, the first uniform mode appears to dominate the response characteristics. It is also noted that the interstory drift decreases with the installation of base-isolation system. On a percentage basis, the wind-induced response of the base-isolated buildings with lower aspect ratio is much greater than that of their fixed counterparts. But the absolute magnitude of these responses is relatively small. In short, both the need for and the effectiveness of the proposed hybrid passive control system increases with increasing building height. Nonetheless, for taller buildings the base isolation concept is not effective and other concerns like stability preclude their usage.

Another objective of this study is to determine the validity of commonly used classical damping assumptions when analyzing the BI, BIBTMD, BI2TMD, and the FXTTMD configurations. The assumption of classical damping is only valid when damping is weak or appropriately distributed. Conventional analysis performed under this assumption neglects the interaction between orthogonal modes. The introduction of concentrated dampers into the system invalidates this assumption by fundamentally changing the distribution of damping in the system. For the sake of illustrations, only the 600 and 150 ft tall buildings are studied in this analysis to examine the implications of a tacit assumption of classical damping. The analysis is carried using conventional modal analysis in which the off-diagonal terms of the generalized damping matrix are ignored and the results are compared to the state-space formulation that does not require that the system be classically damped. It is noted that the assumption of classical damping can lead to rather large errors in the calculated responses of a structure, fixed-base or base-isolated, in the presence of TMDs or other mitigation devices. Tsai and Kelly [15] also observed that the assumption of classical damping seems to be valid for base-isolated structures with no extraneous mitigation or other devices.

The $P-\Delta$ effects for both the superstructure and the rubber bearings were accounted for in the previous two observations due to anticipated deflections of the rubber bearings. The results indicate that neglecting the $P-\Delta$ effects in the super-structure and in the rubber bearings leads to underestimating the actual RMS response for base-isolated buildings. Similar trends were found for other buildings.

A parameter study is performed in order to illustrate the effect of varying various parameters of the building on base-isolation systems. As one would expect, when mass, stiffness and damping are added to the super-structure, the response decreases. The details are omitted here [11]. The effects of changing the stiffness and damping ratio of the base-isolation system are given in Fig. 5. As noted in the case of

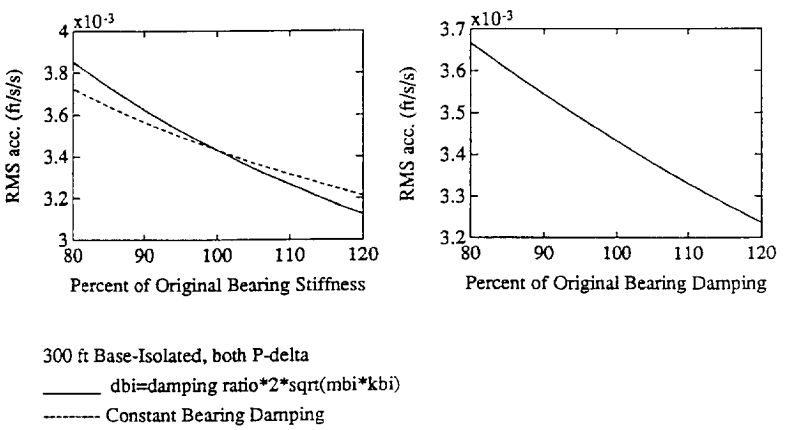

Fig. 5. Effect of isolator stiffness and damping.

super-structure, altering these parameters results in a proportional effect on the response. However, the results of this study show that changes in the base-isolation system parameters, e.g., stiffness and damping have a more pronounced effect on the building response in comparison with the similar alterations in the super-structure. This can be attributed to the fact that inter-storey responses decrease with the addition of a base-isolation system and the building response at the top depends on the isolation stiffness characteristics. It is also noted in Fig. 5 that by increasing the damping capacity of the base-isolation system the sensitivity of base-isolated buildings to wind can be reduced. This can be achieved by utilizing R-FBI of highly damped LRB system.

6. Concluding remarks

In this study the wind-induced response of base-isolated buildings with passive dampers attached to the building base and/or top. A number of conclusions can be drawn from this study:

- The state-space representation of wind velocity fluctuations leads to the simulation of wind field that provides a good match with prescribed spectral description. Combined with system equations, the state-space representation facilitates the dynamic analysis of combined systems which otherwise requires a classical damping assumption or alternative analysis procedures. The analysis presented here can be extended to include other base isolation systems such as the resilient friction base isolator and high damping laminated rubber bearing utilizing equivalent linearization.
- Both the lower and top TMDs aid in mitigating wind induced response, the lower TMD is more effective. Inter-story drift of wind loaded buildings decrease with the installation of a base-isolation system.
- Altering base-isolation bearing parameters such as damping and stiffness has a more pronounced effect on building response than similar changes in the super-structure parameters. It is noted that by increasing the damping capacity the sensitivity of base-isolated buildings to wind can be significantly reduced. This can be achieved by utilizing R-FBI of highly damped LRB systems.
- The analysis of base-isolated buildings can be performed with the assumption of classical damping, but both fixed-base and base-isolated structures with appendages such as TMDs may not be accurately analyzed by the assumption of classical damping.
- The optimal TMD parameters of fixed-base buildings can be determined from previous optimization studies. The introduction of base-isolation fundamentally changes the system, which requires that the optimization of TMD parameters be performed for each individual MDOF base-isolated structural system. A detailed optimization study may provide useful expressions for optimization.

Acknowledgements

The support for this work and preparation of this manuscript was provided by the NSF Grants BCS 90-96274 and CMS 95-03779.

References

[1] J.M. Kelly, Aseismic base-isolation: review and bibliography, Soil Dyn. Earthquake Eng. (5) (1986) 202–216.
[2] L. Su, G. Ahmadi, I.G. Tadbakhsh, Response of base-isolated shear beam structures to random excitations, Probab. Eng. Mech. 5 (1) (1990) 35–46.
[3] P. Henderson, M. Novak, Response of base isolated buildings to wind loading, Earthquake Eng. Struc. Dyn. 18 (8) (1989) 1201–1217.
[4] A. Kareem, M.J. DeKlotz, Dynamics of wind excited base-isolated buildings with passive dampers, Technical Report No. NDCE 91-003, Department of Civil Engineering, University of Notre Dame, Notre Dame, Indiana, 1991.
[5] Y. Chen, G. Ahmadi, Wind effects on base isolated structures, J. Eng. Mech. 118 (8) (1992) 1708–1727.
[6] S.C. Sinha, G. Li, Optimal design of base-isolated structure with dynamic absorbers, J. Eng. Mech. ASCE 120 (2) (1993) 221–231.
[7] J.N. Yang, D. Wong, On aseismic hybrid control system, structural safety and reliability, Proc. ICOSSAR '89, San Francisco, Vol. I, 1989, pp. 471–478.
[8] G.K. Chan, J.M. Kelly, Effects of axial load on elastometric isolation bearings, Report No. EERC 86/12, Earthquake Engineering Research Center, University of Berkeley, November 1987.
[9] G.B. Warburton, Optimum absorber parameters for various combinations of response and excitation parameters, Earthquake Eng. Struct. Dyn. 10 (1982) 381–401.
[10] A. Kareem, Mitigation of wind induced motion of tall Buildings, J. Wind Eng. Ind. Aerodyn. (11) (1983) 273–284.
[11] A. Kareem, Dynamics of base-isolated buildings with passive dampers under winds, Wind Engineering: Retrospect and Prospect, Papers for the 9th Int. Conf. on Wind Engineering, vol. V, Wiley, New Delhi, 1995.
[12] E. Gossmann, H. Waller, Analysis of multi-correlated wind-excited vibrations of structures using the covariance method, Eng. Struc. 5 (1983) 264–272.
[13] J. Suhardjo, R.F. Spencer Jr., A. Kareem, Frequency domain optimal control of wind excited buildings, J. Eng. Mech. ASCE 118 (12) (1992) 2463–2481.
[14] J.M. Maciejowski, Multivariable Feedback Design, Addison-Wesley, NY, 1989, pp. 50–52.
[15] H.-C. Tsai, J.M. Kelly, Non-classical damping in dynamic analysis of base-isolated structures with internal equipment, Earthquake Eng. Struct. Dyn. 16 (1988) 29–43.